Proton-donor properties of water and ammonia in van der Waals complexes. Be–H_2O and Be–NH_3

G. Chałasiński
Department of Chemistry, University of Warsaw, Pasteura 1, 02-093 Warszawa, Poland,[a] Department of Chemistry and Biochemistry, Southern Illinois University, Carbondale, Illinois 62901, and Department of Chemistry, Oakland University, Rochester, Michigan 48309

M. M. Szczęśniak
Department of Chemistry, Oakland University, Rochester, Michigan 48309

S. Scheiner
Department of Chemistry and Biochemistry, Southern Illinois University, Carbondale, Illinois 62901

(Received 16 September 1992; accepted 7 January 1993)

The potential energy surfaces (PES) of Be–H_2O and Be–NH_3 are studied with particular attention to characterization of proton-donor properties of water and ammonia. Calculations were performed by means of both supermolecular and intermolecular Møller Plesset perturbation theory. The Be–H_2O PES reveals two van der Waals minima: the C_{2v} minimum (D_e $=176$ cm^{-1}, $R_e=6.5$ bohr), and the H-bonded minimum ($D_e=161$ cm^{-1}, $R_e=7.5$ bohr), separated by a barrier of 43 cm^{-1} at the T-shaped configuration. The Be–NH_3 PES reveals only one van der Waals minimum, at the C_{3v} configuration ($D_e=260$ cm^{-1}, $R_e=6.5$ bohr) and a saddle point at the H-bonded geometry. The locations of the minima as well as the anisotropy of the interaction are determined by the anisotropy of electric polarization contribution, embodied by the self-consistent-field (SCF)-deformation and perturbation induction energies.

I. INTRODUCTION

Common wisdom about the hydrogen bond suggests that water and ammonia should have basically similar hydrogen bonding capabilities. That is, they both should be able to act as a hydrogen-bond donor and as a hydrogen-bond acceptor. However, whereas this is true for the water molecule, except for the NH_3 dimer, there is so far no known example of the ammonia molecule acting as a proton donor in the gas phase.[1–3]

Elucidation of these anomalous properties of ammonia is important from the broad perspective of the hydrogen bond concept. In this context, analysis of the potential energy surfaces (PES) in the regions where water's and ammonia's protons contact other atoms and molecules is of great interest. In particular, there is a strong incentive to find a strong proton acceptor to which NH_3 might form a donor hydrogen bond.[2]

Our previous studies of a number of complexes formed by Ar and various hydrides, such as Ar–NH_3,[4] Ar–H_2O,[5] Ar–CH_4,[6] and Ar–HCl[7] (see also Ref. 8), seem to indicate that the ability to form a H-bonded structure is related to electric polarization effects, encompassed by the self-consistent-field (SCF)-deformation and induction energies. (By a hydrogen bond we mean here a weakly bound geometrical arrangement with an H atom lying in between other atoms, very much in the spirit of the definition of Pimentel and McClellan.[9]) The induction energy depends upon two factors: high polarizability of the rare gas atom and the strength of the electric field along the X–H bond in the hydride. The experimental evidence seems to be compatible with the above conclusions.

This paper is the second in a series of papers where we investigate van der Waals complexes between ammonia and other species, and compare them with similar complexes of water. In the previous paper we analyzed the Kr–H_2O and Kr–NH_3 systems.[10] Since Kr has a relatively large polarizability (about 17 a.u.[11]) there was some expectation that it might hydrogen bond to ammonia. However, similar to the Ar–NH_3 case,[4] the H-bonded structure proved to be a saddle point, and the global minimum was related to the T-shaped configuration, with the Rg–N axis almost perpendicular to the C_3 axis. The crucial role of electric polarization represented by the SCF-deformation and perturbation induction effects in the formation of the H-bond was confirmed, and essentially weaker polarization properties of N–H bond in NH_3 than O–H bond in H_2O were noticed.

In this paper we present an *ab initio* study of the Be complexes, Be–H_2O and Be–NH_3. The Be atom is known to be unusually prone to electric polarization, its polarizability being about 38 a.u.,[12] i.e., more than twice as large as that of Kr. Therefore, the Be atom seems an excellent candidate to form a hydrogen bond and studying its complexes with water and ammonia may help to elucidate the differences in the hydrogen bonding capabilities between these two molecules. In addition, complexes of Be involving water and ammonia are of potential interest in understanding the reaction mechanisms involving molecules interacting with metal surfaces. Our *ab initio* study employed a combination of the perturbation theory of intermolecular forces[13] with the supermolecular Møller–Plesset perturba-

[a]Permanent address.

 0021-9606/93/097020-09$06.00

tion theory (MPPT).[14,15] This approach has recently been successfully applied to a number of complexes involving rare gases and other molecules.[4–8]

To the best of our knowledge only the Be–H_2O complex was previously investigated and the studies were limited to the global minimum with the Be atom weakly bound to the oxygen atom.[16–18] In 1985 Curtiss and Pople presented *ab initio* MPPT data of the Be–H_2O complex.[16] The results of this study suggested that the Be–H_2O complex is nonplanar, with beryllium lying ca. 55° above the water plane, and with a short Be–O distance of 3.281 bohr and a dissociation energy of 1930 cm^{-1}. In addition, the authors reported also the existence of an outer van der Waals minimum for the coplanar C_{2v} configuration, $R_e = 6.05$ bohr, and a well depth of 240 cm^{-1}. Five years later Haase *et al.*[17] cast doubt on the existence of the inner minimum. Haase *et al.* repeated some of the previous calculations but also corrected for basis set superposition error (BSSE). After correction, the inner minimum disappeared while the outer minimum persisted. The structure of Be–H_2O proved to be planar and of C_{2v} symmetry, with R_e and D_e estimated to be 6.6 bohr and 226 ± 83 cm^{-1}, respectively. This seemed to be the first reliable characterization of the global van der Waals minimum in Be–H_2O. The authors pointed to the necessity of BSSE removal to obtain correct PES. The 6–311G^{**} basis was also shown to be an inadequate basis set to describe this interaction. Recently, Curtiss and Pople reexamined the Be–H_2O complex using extended basis sets and MPPT through the fourth order.[18] Once more both the inner and outer minima were found although the inner minimum turned out less deep than in their previous study. The authors estimated the inner minimum well depth as about 351 cm^{-1} and Be–O distance as about 3.3 bohr. After correcting for BSSE, the well depth is further reduced to 175 cm^{-1}. The conditions under which it was obtained [the minimum appeared only after the geometry relaxation of the water moiety and only with the largest TZ++(3*d*2*f*,3*pd*) basis] suggest that usual intermolecular forces are not enough to explain its origin. As to the outer minimum, its parameters D_e and R_e were found to be 175 cm^{-1} and 6.0 bohr, respectively. The outer minimum appears to be a typical van der Waals minimum. The present work focuses on more comprehensive characterization of the PES of Be–H_2O in the regions where it is governed by common van der Waals forces whereas the inner minimum is given only brief attention.

II. METHOD AND DEFINITIONS

The supermolecular Møller–Plesset perturbation theory (MPPT) interaction energy corrections are derived as the difference between the values for the total energy of the dimer and the sum of the subsystem energies, in every order of perturbation theory

$$\Delta E^{(n)} = E_{AB}^{(n)} - E_A^{(n)} - E_B^{(n)}, \quad n = \text{SCF},2,3,4,\ldots . \tag{1}$$

The sum of corrections through the nth order will be denoted $\Delta E(n)$; thus, e.g., $\Delta E(3)$ will symbolize the sum of ΔE^{SCF}, $\Delta E^{(2)}$, and $\Delta E^{(3)}$. Each individual $\Delta E^{(n)}$ correction can be interpreted[14] in terms of intermolecular Møller–Plesset perturbation theory (IMPPT) which encompasses all well-defined and meaningful contributions to the interaction energy such as electrostatic, induction, dispersion and exchange, and may be expressed in the form of a double perturbation expansion.[13] The IMPPT interaction energy corrections are denoted $\epsilon^{(ij)}$, where i and j refer to the order of the intermolecular interaction operator and the intramolecular correlation operator, respectively (see Ref. 13 for more details).

A. Partitioning of ΔE^{SCF}

ΔE^{SCF} can be dissected as follows (cf. Refs. 14 and 15 for more details)

$$\Delta E^{\text{SCF}} = \Delta E^{\text{HL}} + \Delta E_{\text{def}}^{\text{SCF}}, \tag{2}$$

$$\Delta E^{\text{HL}} = \epsilon_{\text{es}}^{(10)} + \epsilon_{\text{exch}}^{\text{HL}}, \tag{3}$$

where ΔE^{HL} and $\Delta E_{\text{def}}^{\text{SCF}}$ are the Heitler–London and SCF-deformation contributions, respectively. ΔE^{HL} is further divided into the electrostatic, $\epsilon_{\text{es}}^{(10)}$, and exchange, $\epsilon_{\text{exch}}^{\text{HL}}$, components. The SCF deformation originates from mutual electric polarization restrained by the Pauli (antisymmetry) principle.[19,20] Its perturbation approximations, $\epsilon_{\text{ind}}^{(20)}$ and $\epsilon_{\text{ind},r}^{(20)}$ are also considered.

B. Partitioning of $\Delta E(2)$

$$\Delta E^{(20)} = \epsilon_{\text{es},r}^{(12)} + \epsilon_{\text{disp}}^{(20)} + \Delta E_{\text{def}}^{(2)} + \Delta E_{\text{exch}}^{(2)}, \tag{4}$$

$\epsilon_{\text{es},r}^{(12)}$ denotes the second-order electrostatic correlation energy with response effects,[15] and $\epsilon_{\text{disp}}^{(20)}$ the Hartree–Fock dispersion energy. $\Delta E_{\text{def}}^{(2)}$ and $\Delta E_{\text{exch}}^{(2)}$ stand for the second-order deformation correlation correction to the SCF deformation and the second-order exchange correlation, respectively. The latter encompasses the exchange-correlation effects related to electrostatic correlation and dispersion.

C. Calculations of interaction energies

Unless stated otherwise, calculations of all the supermolecular and perturbational interaction terms are performed using the basis set of the entire complex, i.e., dimer-centered basis sets (DCBS).[21,22] This procedure amounts to applying the counterpoise (CP) method of Boys and Bernardi.[23] (Despite long controversy over accuracy of this procedure, recent papers by Yang and Kestner,[24] Tao and Pan,[25] and Cybulski and Chałasinski[26] confirm that the CP technique is very efficient.) To assure the consistency of evaluation of the MPPT and IMPPT interaction energy corrections all the intermolecular perturbation terms $\epsilon^{(ij)}$ must be derived in DCBS as well.

D. Basis sets

Medium-size polarized basis sets of Sadlej[27] were used for H_2O and NH_3.

H_2O: the S basis which is [5*s*3*p*2*d*/3*s*2*p*], and the $S(f,d)$ basis which is the S basis augmented with a single f-symmetry orbital at O (0.18) and a single d-symmetry orbital at H (0.18) (cf. Ref. 5).

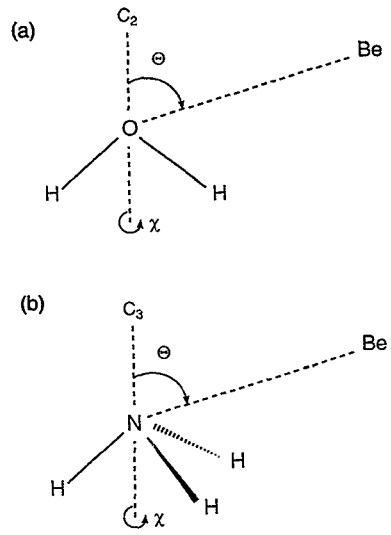

FIG. 1. Geometrical parameters of the complexes: (a) Be–H_2O; $\chi=0°$ corresponds to Be lying in the plane of water, (b) Be–NH_3; $\chi=0°$ corresponds to Be lying in the plane which encompasses the C_3 axis and the H–N bond.

NH_3: the S basis which is [5*s*3*p*2*d*/3*s*2*p*], and the $S(f,d)$ basis which is the S basis augmented with a single f-symmetry orbital at N (0.18) and a single d-symmetry orbital at H (0.14).

For Be several basis sets from the study by Diercksen *et al.*[28] were used, and are named as in their paper: *A*1-[7*s*3*p*2*d*], *D*1-[7*s*3*p*2*d*1*f*], *D*2-[7*s*3*p*2*d*2*f*]. (Note that in contrast to Ref. 28, 5*d* and 7*f* Gaussian orbitals were used.) The largest *D*2 basis was previously found to give almost quantitative agreement of the MP4 interaction energy in the Be dimer with the experimental data.[28]

All results were obtained using GAUSSIAN 90[29] and GAUSSIAN 92[30] programs, and an intermolecular perturbation theory package of Cybulski.[31]

III. RESULTS AND DISCUSSION

A. Characterization of Be–H_2O potential energy surface

The internal geometry of H_2O was assumed to be undistorted by the interaction: the experimental geometry with $r(OH)=0.9572$ Å and $\Theta(HOH)=104.524°$ was the same as in Ref. 32. The scan of the PES was carried out for the coplanar ($\chi=0°$) and perpendicular ($\chi=90°$) motions of the Be atom, cf. Fig. 1(a). The intermolecular distances R ranged from 5.0 to 8.5 bohr, with an increment of 0.5 bohr. Θ varied from 0° to 180° in both the coplanar and perpendicular arrangements.

The scan of the PES revealed the existence of two minima: the global minimum at around $R=6.5$ bohr and $\Theta=0°$, $\chi=0°$, hereafter referred to as the C_{2v} minimum, and a local minimum at around 8.0 bohr and $\Theta=120°$, $\chi=0°$, hereafter referred to as the H-bonded minimum.

To visualize the anisotropy of the interaction, several slices of the PES, calculated at the MP2 level of theory with the *A*1/*S* basis set at several R, are shown in Fig. 2. The angle Θ varies from 0° to 180° (for both coplanar and perpendicular motions) and the values of R are from the range of 6.5 to 8.5 bohr. Within this range of R both the H-bond minimum and the C_{2v} global minimum regions are seen.

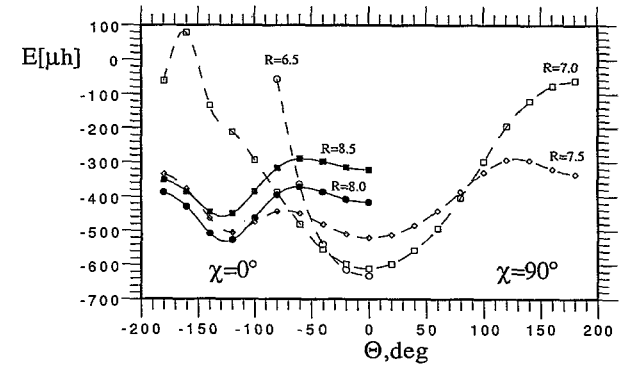

FIG. 2. Θ dependence of the Be–H_2O interaction energy for different R calculated at the MP2 level of theory.

One can see that when Be is moving in the water plane from the C_{2v} minimum to the H-bond minimum, R must increase and a barrier around $\Theta=80°$ (the T configuration) must be overcome. As to the perpendicular motion we should note the decrease of the interaction energy when Be moves toward hydrogens. From the monotonic behavior of the total interaction energy and its components we conclude that Be does not detect any concentration of electronic charge cloud which would correspond to sp^3 lone pairs on O.

The above results and conclusions were obtained with the relatively small basis *A*1/*S* for beryllium and at the lowest correlated level of theory, MP2. In order to confirm our findings as well as to obtain a better quantitative estimate of the minima and the barrier, we performed for selected geometries additional calculations with the most extended *D*2/*S*(*f*,*d*) basis set through the fourth order of MPPT. At the C_{2v} minimum D_e increased from 138.6 cm^{-1} to 162.7 cm^{-1} and 176.3 cm^{-1}, at the MP2 and MP4 levels of theory, respectively. R_e remained about the same, ca. 6.5 bohr. At the H-bond minimum D_e increased from 115.5 cm^{-1} to 127.5 cm^{-1} and 161.8 cm^{-1}, at the MP2 and MP4 level of theory, respectively, and R_e shifted from 8.0 to 7.5 bohr. Finally, the barrier height changed from 41.2 cm^{-1} to 53.2 cm^{-1} and 43.3 cm^{-1}, at the MP2 and MP4 level of theory, respectively, and the related R shifted from 7.5 to 7.0 bohr. From these additional calculations one can conclude that the relative stabilization of the three configurations under consideration as well as the positions of the minima and the saddle point do not qualitatively depend upon the basis set at the MP2 level. They become deeper from about 10 cm^{-1} (H-bond configuration and T configuration) to about 20 cm^{-1} (the C_{2v} configuration), and the H bond and T configurations also shifted by about 0.5 bohr toward smaller R. Similarly, allowing for higher orders at the MP4 level further raises the magnitude of the

TABLE I. Interaction energy components for three configurations of Be–H_2O; R corresponds to the minimum at a given configuration. All energies in μhartree.

	C_{2v} conf.[a]			T conf.[b]			H-bond conf.[c]		
	A1/S	*D2/S*	*D2/S(f,d)*	*A1/S*	*D2/S*	*D2/S(f,d)*	*A1/S*	*D2/S*	*D2/S(f,d)*
					Frozen core				
ΔE^{SCF}	379.3	382.2	380.0	372.1	370.3	372.1	285.8	287.0	283.3
$\Delta E^{(2)}$	−1006.8	−1060.7	−1121.3	−812.7	−835.9	−871.1	−808.9	−828.8	−857.5
$\Delta E(2)$	−627.5	−678.4	−741.3	−440.6	−465.6	−499.0	−523.0	−541.8	−574.3
$\Delta E^{(3)}$	39.6	36.2	31.0	−3.1	−3.5	−4.2	−8.5	−9.3	−7.4
$\Delta E^{(4)}_{DQ}$	126.5	130.6	139.2	71.9	73.5	77.9	71.5	73.8	77.5
$\Delta E^{(4)}_{SDQ}$	94.6	96.2	103.0	50.6	51.9	54.6	45.9	47.5	49.5
$\Delta E^{(4)}$	−77.6	−87.9	−92.9	−74.9	−79.7	−86.5	−85.2	−88.8	−97.1
$\Delta E(4)$	−665.5	−725.8	−803.3	−518.6	−545.4	−589.8	−616.8	−636.5	−678.7
$\Delta E^{CCSD(T)}$		−616.1							
$\Delta E^{QCISD(T)}$		−624.0							
					All electron				
ϵ^{HL}_{exch}	3136.9	3139.0	···	1039.3	1039.4	···	905.7	906.0	···
$\epsilon^{(10)}_{es}$	−1695.2	−1691.0	···	−342.8	−346.0	···	−158.1	−156.0	···
ΔE^{SCF}_{def}	−1062.4	−1065.8	···	−324.4	−324.1	···	−461.8	−463.0	···
$\epsilon^{(20)}_{ind,r}$	−2272.2	−2274.0	···	−848.4	−850.0	···	−810.5	−812.0	···
$\epsilon^{(12)}_{es,r}$	96.0	106.0	···	17.7	21.0	···	−20.9	−19.0	···
$\epsilon^{(20)}_{disp}$	−1727.6	−1777.0	···	−884.0	−900.0	···	−781.9	−792.0	···
$\epsilon^{(21)}_{disp}$	40.3	32.0	···	−14.7	17.0	···	−36.6	−38.0	···

[a] R=6.5 bohr, Θ=0°, χ=0°.
[b] R=7.5 bohr, Θ=80°, χ=0°.
[c] R=8.0 bohr, Θ=120°, χ=0°.

interaction energy by ca. 20 cm^{-1} but does not change our conclusions either. The frozen core approximation only negligibly affected the interaction energies. Here, the MPPT series reveals a reasonable convergence (cf. Table I). The major repulsive and attractive contributions are located in ΔE^{SCF} and $\Delta E^{(2)}$, respectively. The third order is practically negligible. In the fourth order the singles, doubles, and quadruples (SDQ) terms provide some secondary repulsion but eventually the whole term is attractive due to the domination of triples. Such a convergence is quite similar to that observed in the Ar molecule case rather than in the Be_2 case where it is fairly slow.[28,33] In addition, even in the Be_2 case, the MP2 and MP4 levels of theory proved to be very efficient, more efficient than, e.g., various truncated coupled cluster (CC) approximations.[34] Yet, in complexes with Be, notorious for quasidegeneracy in its $2s$–$2p$ shell, one should always take extra care to verify performance and consistency of the results by other correlated methods. Therefore, we also carried out additional CCSD(T) (coupled cluster including single, double, and noniterative triple substitutions[35,36]) and QCISD(T) (quadratic configuration interaction including single, double, and noniterative triple substitutions[36]) calculations with the *D2/S* basis at the global C_{2v} minimum. The results are given in Table I. One can see that CCSD(T) and QCISD(T) provide similar correlation contribution which is smaller by about 22 cm^{-1} than that predicted by MP4. Note that the difference of 22 cm^{-1} amounts to about 10% of the total correlation term, and 15% of the total interaction energy.

Our best estimates of R_e and D_e [MP4 with the *D2/S(f,d)* basis set] are for the C_{2v} minimum 176.3 cm^{-1} at 6.5 bohr, respectively, and for the H-bond minimum 161.8 cm^{-1} at 7.5 bohr, respectively.

The best estimate of the saddle point in the barrier (T configuration, Θ=80° and χ=0°) is 129.4 cm^{-1} at 7.5 bohr. The height of the barrier with respect to the global minimum is thus 43.2 cm^{-1}.

1. Analysis of Be–H_2O interaction anisotropy

The anisotropies of different components of the interaction energy for the coplanar geometry are shown in Fig. 3 (SCF level), Fig. 4 (MP2 level), and in Table II. The anisotropies of the individual components of the SCF interaction energy: electrostatic, exchange, and induction, are similar as in the Ar–H_2O case, In fact, if one compares

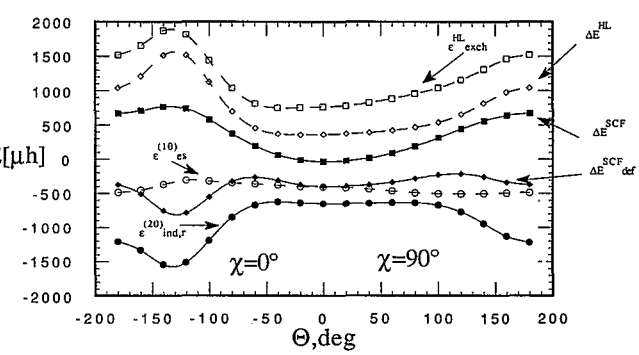

FIG. 3. Θ dependence of the Be–H_2O interaction energy terms which belong to ΔE^{SCF} (for definitions see the text). R is kept at 7.5 bohr.

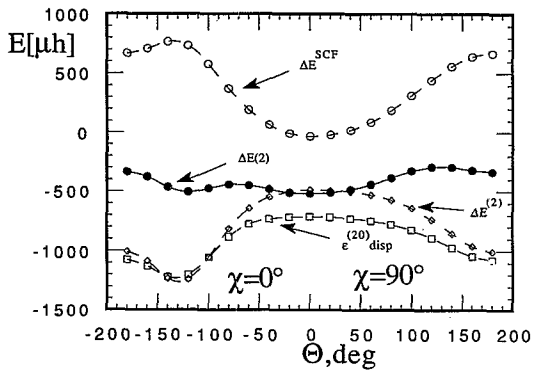

FIG. 4. Θ dependence of the Be–H_2O interaction energy terms involving correlation (for definitions see the text). R is kept at 7.5 bohr.

the corresponding figure for Ar–H_2O (Fig. 3 in Ref. 5) at first sight one finds no difference whatsoever. There is, however, one important quantitative difference: the electric polarization plays a substantially greater role in the case of Be–H_2O. It is visualized by a relatively large contribution from the SCF deformation and $\epsilon^{(20)}_{\mathrm{ind},r}$, which are much larger than in the Ar–H_2O case: ten times and four times as large at the C_{2v} and H-bond configurations, respectively. This makes the total SCF interaction energy curve much flatter which enables formation of two minima at the correlated level.

The behaviors of the various post-SCF terms are illustrated in Fig. 4 (see also Table II). First, one can see that the anisotropy of the dispersion, the major contribution to $\Delta E^{(2)}$, is reciprocal to the exchange energy (cf. Fig. 4), and therefore to the SCF interaction energy. The behavior of the total $\Delta E^{(2)}$ reflects qualitatively the shape of $\epsilon^{(20)}_{\mathrm{disp}}$ although some modification of anisotropy is due to the second order exchange terms. Although qualitative behavior of individual components: electrostatic, exchange, electric polarization, and dispersion in both the Be–H_2O and Ar–H_2O systems are very similar, the anisotropy of the total PES at the MP2 level of theory is completely different. Ar–H_2O revealed one broad van der Waals minimum for Θ ranging from 80° to 120°. Be–H_2O has a barrier in this region which separates two minima, at 0° and 120°. This feature is due to the much larger role of the SCF-deformation energy which is also strongly anisotropic. In fact, $\Delta E^{\mathrm{SCF}}_{\mathrm{def}}$ is almost as large as the dispersion energy for both the global and local minima, cf. Table I. This is a striking contrast to the general case of van der Waals complexes that include rare gas atoms and molecules where the SCF-deformation and perturbation induction terms are typically an order of magnitude smaller than the dispersion term. A qualitatively important role of the SCF-deformation energy (and to some extent the electrostatic energy) for the C_{2v} configuration appears to be a characteristic feature of the Be–H_2O complex. Although surprising it is not unexpected. The Be atom has an unusually large polarizability and a diffuse electronic charge cloud. In the Be dimer there was also a large and crucial contribution from $\Delta E^{\mathrm{SCF}}_{\mathrm{def}}$, which shifted the minimum to considerably shorter distances.[37] One may say that the shape of Be–H_2O PES reflects and is governed by the induction anisotropy. With this peculiarity the outer minima in Be–H_2O seem to be a classical van der Waals type of minima.

2. Inner minimum problem

In this study we are interested primarily in the outer minimum since it appears to be a common type of van der Waals minimum. As to the inner minimum its origin and

TABLE II. Θ dependence of the interaction energy terms for Be–H_2O at $R=7.5$ bohr, the $A1/S$ basis set (for definitions, see the text). Energies in μhartree.

Θ[°]	$\epsilon^{(10)}_{\mathrm{es}}$	$\epsilon^{\mathrm{HL}}_{\mathrm{exch}}$	ΔE^{HL}	ΔE^{SCF}	$\epsilon^{(12)}_{\mathrm{es},r}$	$\epsilon^{(20)}_{\mathrm{disp}}$	$\Delta E^{(2)}$	$\Delta E(2)$	$\Delta E^{\mathrm{SCF}}_{\mathrm{def}}$	$\epsilon^{(20)}_{\mathrm{ind},r}$
					Coplanar, $\chi=0°$					
0	−403.3	766.4	363.2	−32.5	32.1	−715.3	−487.0	−520.5	−395.7	−645.5
20	−395.7	756.1	360.4	−8.4	31.4	−717.9	−501.5	−509.8	−368.8	−633.9
40	−377.1	748.6	371.5	65.8	30.1	−731.7	−547.2	−481.4	−305.7	−620.1
60	−358.6	812.7	454.1	192.8	27.6	−777.2	−643.2	−450.4	−261.3	−664.4
80	−342.8	1039.3	696.6	372.1	17.7	−884.1	−816.1	−444.0	−324.5	−848.4
100	−317.0	1443.7	1126.7	578.2	−9.6	−1052.9	−1053.6	−475.4	−548.5	−1191.4
120	−305.5	1822.5	1517.0	734.7	−46.6	−1202.2	−1239.8	−505.0	−782.2	−1511.5
140	−364.5	1881.4	1516.9	767.4	−59.1	−1219.8	−1231.8	−464.4	−749.5	−1540.0
160	−450.3	1662.5	1221.2	708.8	−42.0	−1130.1	−1806.0	−377.2	−503.3	−1330.8
180	−483.9	1524.4	1040.5	669.9	−30.3	−1075.0	−1004.6	−334.7	−370.5	−1207.2
					Perpendicular, $\chi=90°$					
20	−411.9	782.4	370.4	−19.9	29.9	−718.1	−491.5	−511.4	−390.4	−644.5
40	−434.6	825.3	390.7	19.1	23.6	−728.0	−504.0	−484.9	−371.6	−640.4
60	−463.0	884.8	421.9	88.0	13.8	−747.6	−529.9	−441.9	−333.9	−633.3
80	−487.2	954.6	467.4	188.3	1.8	−779.6	−574.2	−385.9	−279.1	−633.3
100	−501.3	1040.6	539.3	313.0	−10.2	−826.5	−641.9	−328.9	−226.3	−666.7
120	−504.6	1158.8	654.1	444.4	−19.6	−891.5	−737.1	−292.6	−209.7	−767.3
140	−499.3	1312.4	813.1	560.3	−25.7	−971.9	−854.2	−294.0	−252.9	−940.8
160	−489.3	1460.5	971.1	640.7	−29.2	−1044.9	−960.6	−319.9	−330.4	−1125.3

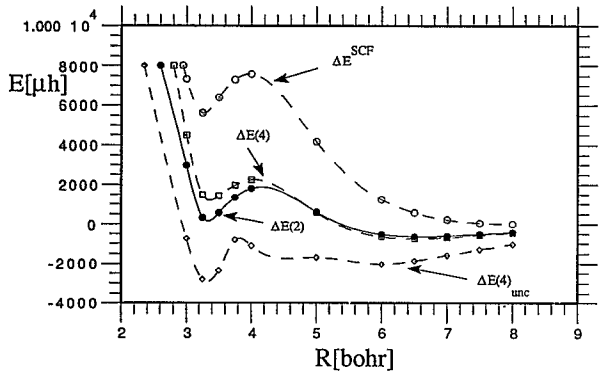

FIG. 5. R dependence of the Be–H_2O interaction energy at the C_s bent configuration, $\Theta=55°$, $\chi=90°$ calculated at different levels of theory.

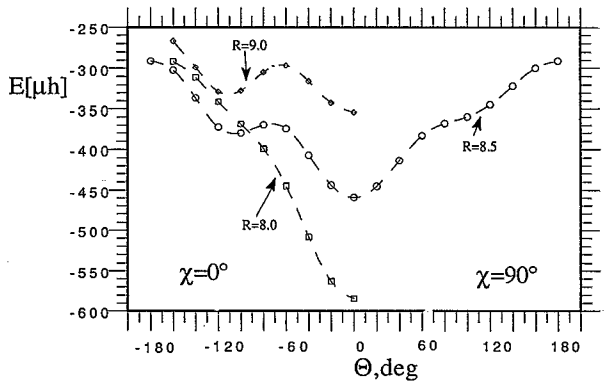

FIG. 6. Θ dependence of the Be–NH_3 interaction energy for different R calculated at the MP2 level of theory.

characteristics remain unclear. According to Curtiss and Pople[18] it appeared only for their largest basis set, TZ++(3*d*2*f*,2*pd*) and only if both the inter- and intramolecular geometries were optimized [they reported that the geometry of the water molecule changed: r(OH) and Θ(HOH) increase by 0.003 bohr and 3.9°, respectively]. From the results of Ref. 18 one can see that the convergence of the MPPT series is different at the inner and outer minima. At the inner minimum the MP4 result is half as deep as the MP2 result. On the contrary, for the van der Waals outer minima and larger distances it is the MP4 result which is substantially deeper.

In order to get some insight into the inner minimum problem we performed calculations with our best *D*2/*S*(*f*,*d*) basis set at the MP4 level of theory. The geometry of water was not optimized, the angles fixed at $\Theta=55°$, $\chi=90°$, and we varied R from 1.5 to 9.0 bohr. (Note that rigorous geometry optimization would be tricky since one should correct for BSSE both inter and intramonomer energies). The MP2 and MP4 interaction energies are plotted in Fig. 5. A few things are worthwhile to note here. First, in the repulsive region the curves differ from typical van der Waals curves in that in the beginning they do not rise very steeply. However, around $R=4.0$ bohr there is an abrupt change in the SCF curve which exhibits unexpected maximum, then it has a minimum around 3.5 bohr and finally rises extremely steeply. These peculiarities are followed by similar ones of the MP2 and MP4 results. First, the MP4 curve crosses and goes above the MP2 curve, and then around 3.0 bohr both the curves begin to rise extremely steeply. One can also see that the CP-uncorrected result $\Delta E(4)_{unc}$ provides unreliable image of the minimum region. These strange results may suggest that there exists another, excited state of the Be–H_2O complex which comes at around 3.0 bohr close to the ground state or even intersects it. At this point, let us invoke the peculiar beryllium dimer ground state which may be interpreted as a result of avoided crossing between two hypothetical diabatic curves: one dissociating into the $2s^2(^1S)$ atoms and the other into $2s2p(^3P)$ atoms.[38] If similar problems occur here, however, then single reference MPPT (as well as coupled cluster or quadratic CI methods) may no longer be adequate to evaluate the interaction energy in this region. To summarize, the existence and characterization of the inner minimum requires further studies, beyond the MPPT approximation and consideration of excited states seems to be necessary. In this paper we are not in a position to solve this problem.

B. Characterization of Be–NH_3 potential energy surface

The geometrical parameters of the Be–NH_3 complex are shown in Fig. 1(b). The internal geometry of NH_3 was assumed to be undistorted by the interaction: the experimental geometry with r(NH)=1.0124 Å and Θ(HNH) =106.67° was the same as in Ref. 39. The values of R under consideration ranged from 5.5 to 9.0 bohr, with an increment of 0.5 bohr. Θ varied from 0° to 180°, and two values of χ were considered, 0° and 60°. $\chi=0°$ corresponds to the motion of Be in the plane encompassing the C_3 axis and the dissection of the HNH angle.

A scan of the PES revealed the existence of only one minimum. This minimum occurs for the Be atom lying at the C_3 symmetry axis and facing the N atom. It is hereafter referred to as the C_{3v} minimum.

The total interaction energy curves $\Delta E(2)$ calculated at 8.0, 8.5, and 9.0 bohr, are visualized in Fig. 6. One can see that for $\chi=0°$ and larger R, cf. 9.0 bohr, there are two valleys, separated by a barrier, which correspond to the C_{3v} configuration and H-bond configuration. With decreasing R, cf. 8.5 bohr, the H-bond valley flattens and the barrier is reduced, to finally disappear, cf. 8.0 bohr, in the slope of the deeper C_{3v} valley. As to the T configuration (which is optimal for Ar–NH_3 and Kr–NH_3) for $R=8.5$ bohr it is higher in energy than the C_{3v} configuration and also than the H-bond configuration at angles Θ larger than 80°. The anisotropies of the three individual SCF energy components: electrostatic, exchange, and induction, are illustrated in Table III and Fig. 7. They qualitatively very much resemble the anisotropy of the same terms in the Ar–NH_3 case.[4] However, the relative roles of these terms are essentially different: the electric polarization terms (ΔE_{def}^{SCF} and $\epsilon_{ind,r}^{(20)}$) as well as the electrostatic term are

TABLE III. Θ dependence of the interaction energy terms for Be–NH_3 at $R=8.5$ bohr, the $A1/S$ basis set (for definitions, see the text). Energies in μhartree.

Θ[°]	$\epsilon_{es}^{(10)}$	ϵ_{exch}^{HL}	ΔE^{HL}	ΔE^{SCF}	$\epsilon_{es,r}^{(12)}$	$\epsilon_{disp}^{(20)}$	$\Delta E^{(2)}$	$\Delta E(2)$	ΔE_{def}^{SCF}	$\epsilon_{ind,r}^{(20)}$
					$\chi=0°$					
0	−176.7	349.6	172.9	−89.1	3.7	−493.7	−370.1	−459.2	−262.0	−306.2
20	−170.4	341.5	171.1	−66.2	3.8	−494.1	−377.8	−444.0	−237.3	−286.7
40	−156.0	334.2	178.2	−0.6	4.7	−501.7	−406.1	−406.7	−178.8	−244.5
60	−143.6	366.7	223.7	95.4	6.3	−534.4	−469.5	−374.0	−127.7	−220.2
80	−140.3	472.9	332.6	206.1	5.7	−607.9	−575.4	−369.3	−126.5	−249.3
100	−149.8	616.9	467.1	301.7	−0.4	−696.3	−681.6	−379.9	−165.4	−311.4
120	−174.6	681.3	506.7	337.1	−9.1	−733.6	−710.2	−372.2	−168.8	−328.0
140	−196.6	623.0	426.4	314.2	−13.8	−701.0	−651.0	−336.8	−112.2	−276.3
160	−201.8	537.7	335.9	276.8	−15.7	−652.4	−579.1	−302.3	−59.1	−219.8
180	−201.8	507.9	306.1	262.7	−16.8	−634.9	−553.5	−290.8	−43.4	−201.0
					$\chi=60°$					
20	−170.0	338.8	168.8	−68.6	3.7	−492.8	−376.5	−445.1	−237.4	−286.4
40	−152.3	311.2	158.9	−18.5	4.4	−490.8	−394.7	−413.2	−177.4	−240.7
60	−132.0	287.8	155.8	42.4	6.4	−494.1	−425.6	−383.2	−113.4	−199.7
80	−120.9	298.4	177.5	104.7	9.1	−514.7	−472.3	−367.6	−72.8	−187.8
100	−128.8	359.7	230.9	169.2	8.8	−557.6	−528.6	−359.4	−61.7	−204.6
120	−154.7	448.8	294.1	229.2	2.4	−608.7	−573.9	−344.7	−64.9	−226.1
140	−183.5	511.6	328.1	265.2	−7.3	−641.1	−586.8	−321.6	−62.9	−228.4
160	−199.1	519.8	320.7	269.1	−14.7	−642.7	−569.0	−299.8	−51.6	−212.4

much larger than in the Ar–NH_3 case. Consequently, the anisotropy of the ΔE^{SCF} interaction energy for Be–NH_3 is qualitatively different from that in Ar–NH_3. In the latter case, at $\Theta=0°$, there is a barrier (since exchange effects prevail) whereas in the former case a valley which leads to a minimum (because of the importance of electric polarization encompassed by the SCF deformation).

The anisotropies of the post-SCF contributions are shown in Table III and Fig. 8. Similar to the SCF level, at the MP2 level of the anisotropies of individual components: $\epsilon_{disp}^{(20)}$, and $\epsilon_{es,r}^{(12)}$, very much resemble those for Ar–NH_3. In particular, the dispersion term has a deep valley for the H-bond configuration and a very shallow one for the C_{3v} configuration. The latter is further smoothed out by the second order exchange effects included in $\Delta E^{(2)}$. The total anisotropy is, however, different and largely determined by the anisotropy of ΔE^{SCF}.

Concluding, there is only one minimum on the PES at the C_{3v} configuration, around $R=6.5$ bohr. The best estimate of D_e is 261.0 cm^{-1}. It was obtained at the MP4 level with the $D2/S(f,d)$ basis set, cf. Table IV.

The nature of the Be–NH_3 interaction at different configurations is compared in Table IV. We compare the interaction energies at the radial minima for three different structures: C_{3v}, H bond and T. One can see that the C_{3v} structure has very large attractive contributions of comparable size, from dispersion, electrostatic, and SCF-deformation effects. On the other hand, the H bond and T structures are predominantly bound by dispersion effects, the other two being small.

Whereas the anisotropies of the elementary components do not qualitatively change with R, it should be

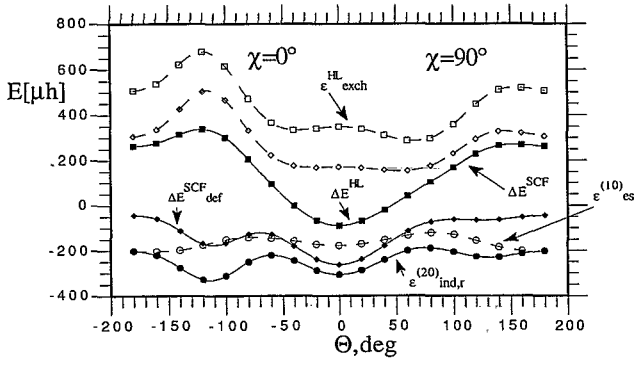

FIG. 7. Θ dependence of the Be–NH_3 interaction energy terms which belong to ΔE^{SCF} (for definitions see the text). R is kept at 8.5 bohr.

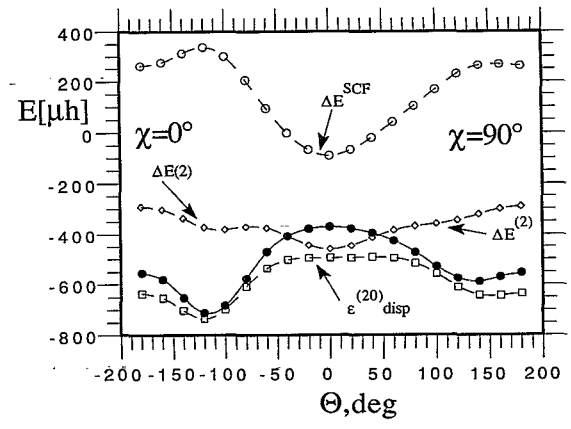

FIG. 8. Θ dependence of the Be–NH_3 interaction energy terms involving correlation (for definitions see the text). R is kept at 8.5 bohr.

TABLE IV. Interaction energy components for three configurations for Be–NH_3; R corresponds to the minimum at a given configuration. (Basis set $A1/S$, all electron calculations, energies in μhartree.)

	C_{3v} conf.[a]			
	$A1/S$	$D2/S(f,d)$	Tconf.[b]	H-bond conf.[c]
ΔE^{SCF}	552.5	531.5	502.8	337.9
$\Delta E^{(2)}$	−1481.5	−1665.5	−996.1	−710.2
$\Delta E^{(3)}$	64.0	50.9		
$\Delta E^{(4)}_{DQ}$	213.4	236.8		
$\Delta E^{(4)}_{SDQ}$	173.1	192.2		
$\Delta E^{(4)}$	−85.9	−106.1		
ϵ^{HL}_{exch}	5300.6		1232.9	681.3
$\epsilon^{(10)}_{es}$	−2896.7		−507.8	−174.6
ΔE^{SCF}_{def}	−1851.4		−172.7	−168.8
$\epsilon^{(20)}_{ind}$	−2428.2		−593.5	−252.4
$\epsilon^{(20)}_{ind,r}$	−2993.9		−738.7	−328.0
$\epsilon^{(12)}_{es,r}$	33.8		28.1	−9.1
$\epsilon^{(20)}_{disp}$	−2619.7		−1168.9	−733.6
$\Delta E(2)$	−928.1	−1134.0	−493.3	−372.2
$\Delta E(4)$	−950.0	−1189.1		

[a] R=6.5 bohr, Θ=0°, χ=0°.
[b] R=7.5 bohr, Θ=80°, χ=60°.
[c] R=8.5 bohr, Θ=120°, χ=0°.

stressed that the anisotropy of the total PES is very much R dependent and our discussion is valid for the region of van der Waals minima. For smaller R, in the repulsive region the anisotropy of the exchange repulsion will be the major factor and PES will be shaped by ϵ^{HL}_{exch}: it will have a valley at the T configuration and barriers at the N end and H end of ammonia. On the other hand, for large R the PES will follow the long range terms, $\epsilon^{(20)}_{ind,r}$ and $\epsilon^{(20)}_{disp}$: with valleys at the H ends and the C_3 axis and a ridge in between. Additional calculations at R=11.0 bohr confirmed this picture and also proved that the H-bond valley is slightly deeper than the C_{3v} valley.

IV. SUMMARY AND CONCLUSIONS

The Be–H_2O ground state PES reveals two minima: the global, C_{2v} minimum, and the local H-bonded minimum. The C_{2v} minimum has a well depth of 176 cm^{-1} and R_e=6.5 bohr. The H-bond minimum has a well depth of 161 cm^{-1}, at R=7.5 bohr. They are separated by a ridge with a saddle point at R of about 7.5 bohr and Θ=80°. The height of the barrier from the bottom of the minimum to the saddle point is estimated as 43 cm^{-1}. It is difficult to assign error bars to those estimates as Be complexes may be different from well documented Ar-molecule complexes. However, the pattern of convergence through the fourth order is remarkably similar. Therefore, assuming similar convergence, the true values of D_e are expected to be larger because of basis set unsaturation of dispersion by 15%–25%. We also attempted to locate the so called "inner" minimum, predicted by Curtiss and Pople[18] for the C_s configuration with the Be atom situated above the H_2O plane. Although we did not find any minimum, we encountered some problems with characterization of the region of the hypothetical minimum by means of MP4 theory. This fact warrants future investigations which would ensure accurate treatment of electron correlation possibly in the vicinity of an excited state of Be–H_2O.

The anisotropies of individual components of the interaction energy: electrostatic, exchange, electric polarization, and dispersion, are qualitatively similar to those for the Rg–H_2O complexes. However, the anisotropy of the total PES qualitatively differs. Instead of a broad minimum for the T configuration, a barrier is found which separates two minima, at the C_{2v} and H-bonded configurations. These differences are due to a very large electric polarization component encompassed by the SCF-deformation and perturbation-induction terms. The electric polarization term stabilizes the H-bonded and C_{2v} configurations since the SCF-deformation and perturbation-induction terms exhibit distinct minima at these configurations.

The Be–NH_3 PES reveals only one minimum, at the C_{3v} configuration. It has a well depth of 260 cm^{-1} and occurs at R_e=6.5 bohr. The anisotropies of elementary interaction energy components very much resemble those for the Rg–NH_3 complexes. However, the anisotropy of the total PES is qualitatively different. The T configuration (which gives a global minimum for Rg–NH_3)is relatively high in energy. On the other hand, the C_{3v} configuration gives a global minimum (while it was a ridge in the Rg–NH_3 case). As in the complexes with water, the differences between Rg and Be complexes are due to large electric polarization of Be which stabilizes the C_{3v} configuration. The electric polarization also stabilizes the H-bond structure but to a lesser extent than in Be–H_2O and not sufficiently to create a local minimum. Be–NH_3 appears to be more stable than Be–H_2O by about 100 cm^{-1}. This reflects more "basic" character of the ammonia molecule.

ACKNOWLEDGMENTS

This work was supported by the National Institutes of Health (GM36912) and by the Polish Committee for Scientific Research KBN Grant No. 2 0556 91 01.

[1] C. A. Schmuttenmaer, R. C. Cohen, J. G. Loeser, and R. J. Saykally, J. Chem. Phys. **95**, 9 (1991).
[2] I. I. Suni, S. Lee, and W. Klemperer, J. Phys. Chem. **95**, 2859 (1991).
[3] J. W. I. van Bladel, A. van der Avoird, P. E. S. Wormer, and R. J. Saykally, J. Chem. Phys. **97**, 4750 (1992); J. G. Loeser, C. A. Schmuttenmaer, R. C. Cohen, M. J. Elrod, D. W. Steyert, R. J. Saykally, R. E. Bumgarner, and G. A. Blake, *ibid.* **97**, 4727 (1992).
[4] G. Chałasiński, S. M. Cybulski, M. M. Szczęśniak, and S. Scheiner, J. Chem. Phys. **91**, 7809 (1989).
[5] G. Chałasiński, M. M. Szczęśniak, and S. Scheiner, J. Chem. Phys. **94**, 2807 (1991).
[6] M. M. Szczęśniak, G. Chałasiński, and S. M. Cybulski, J. Chem. Phys. **96**, 463 (1992).
[7] G. Chałasiński, M. M. Szczęśniak, and B. Kukawska-Tarnawska, J. Chem. Phys. **94**, 6677 (1991).
[8] G. Chałasiński and M. M. Szczęśniak, Croat. Chem. Acta **65**, 17 (1992).
[9] G. C. Pimentel and A. L. McClellan, *The Hydrogen Bond* (Freeman, San Francisco, 1960).
[10] G. Chałasiński, M. M. Szczęśniak, and S. Scheiner, J. Chem. Phys. **97**, 8181 (1992).
[11] R. R Teachout and R. T Pack, At. Data **3**, 195 (1971).
[12] H. J. Werner and W. Meyer, Phys. Rev. A **13**, 13 (1976).
[13] S. Rybak, B. Jeziorski, and K. Szalewicz, J. Chem. Phys. **95**, 6576 (1991).

[14] G. Chałasiński and M. M. Szczęśniak, Mol. Phys. **63**, 205 (1988).
[15] (a) R Moszyński, S. Rybak, S. M. Cybulski, and G. Chałasiński, Chem. Phys. Lett. **166**, 609 (1990); (b) S. M. Cybulski, G. Chałasiński, and R. Moszyński, J. Chem. Phys. **92**, 4357 (1990).
[16] L. A. Curtiss and J. A. Pople, J. Chem. Phys. **82**, 4230 (1985).
[17] F. Hasse, J. Sauer, and V. Kellö, Chem. Phys. Lett. **174**, 19 (1990).
[18] L. A. Curtiss and J. A. Pople, Chem. Phys. Lett. **185**, 159 (1991).
[19] M. Gutowski and L. Piela, Mol. Phys. **64**, 943 (1988).
[20] M. Jeziorska, B. Jeziorski, and J. Cižek, Int. J. Quantum Chem. **32**, 149 (1987).
[21] J. H. van Lenthe, J. G. C. M. van Duijneveldt-van de Rijdt, and F. B. van Duijneveldt, Adv. Chem. Phys. **69**, 521 (1987).
[22] G. Chałasiński and M. Gutowski, Chem. Rev. **88**, 943 (1988).
[23] S. F. Boys and F. Bernardi, Mol. Phys. **19**, 553 (1970).
[24] J. Yang and N. R. Kestner, J. Phys. Chem. **95**, 9214 (1991); *ibid.* **95**, 9221 (1991).
[25] F Tao and Y. Pan, J. Phys. Chem. **95**, 3582 (1991); *ibid.* **95**, 9811 (1991); *ibid.* **96**, 5815 (1992).
[26] S. M. Cybulski and G. Chałasiński, Chem. Phys. Lett. **197**, 591 (1992).
[27] A. J. Sadlej, Coll. Czech. Chem. Commun. **53**, 1995 (1988).
[28] G. H. F. Diercksen, V. Kellö, and J. Sadlej, Chem. Phys. **96**, 59 (1985).
[29] GAUSSIAN 90, M. J. Frisch, M. Head-Gordon, G. W. Trucks, J. B. Foresman, H. B. Schlegel, K. Raghavachari, M. A. Robb, J. S. Binkley, C. Gonzales, D. J. Defrees, D. J. Fox, R. A. Whiteside, R. Seeger, C. F. Melius, J. Baker, R. L. Martin, L. R. Kahn, J. J. P. Stewart, S. Topiol, and J. A. Pople, Gaussian, Inc., Pittsburgh, PA, 1990.
[30] GAUSSIAN 92, M. J. Frisch, G. W. Trucks, M. Head-Gordon, P. M. W. Gill, M. W. Wong, J. B. Foresman, B. G. Johnson, H. B. Schlegel, M. A. Robb, E. S. Replogle, R. Gomperts, J. L. Andres, K. Raghavachari, J. S. Binkley, C. Gonzalez, R. L. Martin, D. J. Fox, D. J. Defrees, J. Baker, J. J. P. Stewart, and J. A. Pople, Gaussian, Inc., Pittsburgh PA, 1992.
[31] S. M. Cybulski, Trurl package, Carbondale IL, 1990.
[32] Experimental parameters taken from G. H. F. Diercksen, B. O. Roos, and A. J. Sadlej, Int. J. Quantum Chem. **S17**, 265 (1983).
[33] R. J. Harrison and N. C. Handy, Chem. Phys. Lett. **95**, 386 (1983).
[34] I. Cernusak, J. Noga, G. H. F. Diercksen, and A. J. Sadlej, Chem. Phys. **125**, 255 (1988).
[35] M. Urban, J. Noga, S. J. Cole, and R. J. Bartlett, J. Chem. Phys. **83**, 4041 (1985); J. Noga and R. J. Bartlett, *ibid.* **86**, 7041 (1987).
[36] J. A. Pople, M. Head-Gordon, and K. Raghavachari, J. Chem. Phys. **87**, 5968 (1987).
[37] G. Chałasiński, Chem. Phys. **82**, 207 (1983).
[38] W. Kutzelnigg, in *Theoretical Models of Chemical Binding, Part 2, The Concept of Chemical Bond*, edited by Zb. Maksić (Springer, Berlin, 1990).
[39] A. J. Sadlej, Mol. Phys. **57**, 509 (1986).